Int. J. of GEOMATE, March, 2014, Vol. 6, No. 1 (Sl. No. 11), pp. 749-756
Geotech., Const. Mat. and Env., ISSN:2186-2982(P), 2186-2990(O), Japan

INVESTIGATION OF STRESS REDUCTION EFFECT ON STRUCTURES DUE TO BASEMAT UPLIFT USING ENERGY CONCEPT

Takafumi Inoue[1] and Atsushi Mikami[2]

[1]Graduate School of Advanced Technology and Science, The University of Tokushima, Japan;
[2]Institute of Technology and Science, The University of Tokushima, Japan

ABSTRACT: This paper studies stress reduction effects induced on structures (such as bridge piers) due to basemat uplift and soil yielding by the use of a macro-element model for foundations placed on sand. A foundation-soil system is modeled as four cases; (1) fixed base, (2) elastic soil, (3) elastic soil with basemat uplift and (4) elasto-plastic soil with basemat uplift. Time histories with different frequency characteristics are considered as input motions to the models. Comparisons of responses of the models show a remarkable reduction of section force due to basemat uplift and soil yielding, depending on characteristics of input motions. Regarding the case where degree of stress reduction effect is largest, energy balance for the system is estimated. In this case, the input energy imparted to the structure by an earthquake tends to be reduced due to the effect of basemat uplift.

Keywords: Bridge Pier, Stress Reduction Effect, Basemat Uplift, Macro-element, Energy

1. INTRODUCTION

As design methods shift to performance-based design, it becomes more important to accurately estimate the response of superstructures accompanied by foundation rotation and basemat uplift. Basemat uplift is reportedly induced even by weak and/or medium ground motions [1], hence, it is necessary to incorporate the effect of basemat uplift into a design code.

Hayashi [2] assessed slightly damaged buildings standing on the most severely damaged area during the 1995 Hyogoken-Nanbu Earthquake. By using numerical simulation, he has studied damage reduction effect due to basemat uplift of buildings which were subjected to strong ground motions, and showed that the damage reduction effect sometimes becomes remarkable depending on structural parameters and input motions. The finite element model was used in his analysis treating soil as a linear or equivalent linear medium.

Iwashita *et al.* [3] examined the effect of uplift at pile head on structural response. They discussed the input energy imparted to structures by an earthquake. They have treated the ground as a kind of spring and assumed that the spring doesn't resist tensile force in order to take the effect of uplift into account.

The authors have studied the reduction effect of a section force induced on structures due to basemat uplift and soil yielding by the use of a macro-element model and showed that the degree of base shear reduction depends on the frequency characteristics of input motions relative to the system [4].

This paper studies the reduction effect of a section force induced in the structure due to basemat uplift and soil yielding from a viewpoint of energy by the use of a macro-element model for foundations placed on sands. A foundation-soil system is modeled as four cases; (1) fixed base, (2) elastic soil, (3) elastic soil with basemat uplift and (4) elasto-plastic soil with basemat uplift. Time histories with different frequency characteristics are considered as input motions in the model.

2. MACRO-ELEMENT MODEL

In this study, a macro-element model developed by Nakatani *et al.* [5] is employed to study stress reduction effect of structures due to basemat uplift and soil yielding. A brief overview is described in this section. Details can be referred to in Shirato *et al.* [6].

2.1 Relationship between Displacements and Loads of a Macro-element Model

In the macro-element model, the foundation is assumed to be rigid, and foundation-soil model which is subjected to combined loads is modeled as one element. Displacements and loads at the center of the footing are defined as shown in Fig. 1 and the following equations.

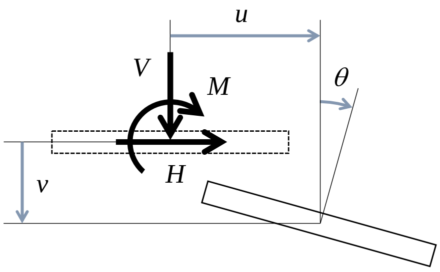

Fig. 1 Definition of displacements and loads for the macro-element model

$$x = \begin{pmatrix} v & u & \theta \end{pmatrix}^T$$
(1)

$$F = \begin{pmatrix} V & H & M \end{pmatrix}^T$$
(2)

where the superscript T stands for transposition. The relationship between incremental displacements and loads is expressed by

$$dF = \left(D^{el} + D^{up} + D^{pl}\right)^{-1} dx$$
(3)

where D^{el}, D^{up} and D^{pl} are elastic compliance, uplift compliance and plastic compliance, respectively.

2.2 Elastic Compliance

In order to determine elastic compliance, equivalent elastic spring coefficients corresponding to the vertical, translational, and rocking component suggested by Gazetas [7] are used. The coefficients for a rectangular foundation are expressed by

$$K_v = \frac{4.54G(B/2)}{1-\nu}$$
(4)

$$K_h = \frac{9G(B/2)}{2-\nu}$$
(5)

$$K_r = \frac{3.6G(B/2)^3}{1-\nu}$$
(6)

where G and ν are shear modulus and Poisson's ratio of the underlying soil and B is the footing length. Frequency dependence of the coefficients is ignored.

2.3 Uplift Compliance

Uplift compliance is determined based on the following model for uplift. The $\theta^{up} - M$ relationship is expressed by

$$\theta^{up} = 0 \; \left(M \le M_\alpha\right)$$
(7)

$$\theta^{up} = \left\{\frac{4}{\left(3 - M/M_\alpha\right)^2} - \frac{M}{M_\alpha}\right\}\theta_0 \; \left(M > M_\alpha\right)$$
(8)

where M_α and θ_0 are moments that are influenced by soil plasticity and rotation at which the uplift initiates. Then the $v^{up} - M$ relationship is expressed by

$$v^{up} = 0 \; \left(M \le M_\alpha\right)$$
(9)

$$v^{up} = -\frac{B}{2}\left\{\frac{4}{\left(3 - M/M_\alpha\right)^2} - \frac{4}{\left(3 - M/M_\alpha\right)} + 1\right\} \; \left(M > M_\alpha\right)$$
(10)

2.4 Plastic Compliance

Plastic compliance is also need to be determined by using bearing capacity surface. A schematic diagram of this is shown in Fig. 2. Shirato *et al*. [6] assumed the following expression for bearing capacity surface.

$$f_{cr} = h^2 + m^2 - \xi^2\left(1-\xi\right)^{2\zeta} = 0$$
(11)

where $\xi = V/V_m$, $h = H/\left(\mu V_m\right)$, $m = M/\left(\psi B V_m\right)$

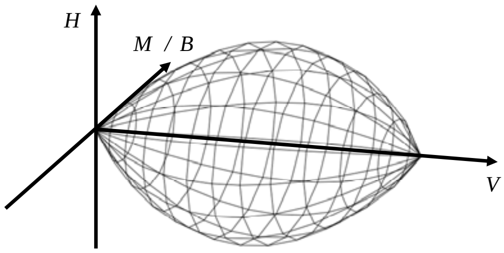

Fig. 2 Schematic diagram of bearing capacity surface

and V_m is bearing capacity in terms of centered vertical loading. Parameters μ and ψ are tangents at the origin on the $V-H$, $V-M$ planes, respectively. To describe plastic deformations, a yield function is defined based on Nova and Montrasio [8] as follows:

$$f_y = h^2 + m^2 - \xi^2 (1 - \xi / \rho_c)^{2\zeta} = 0$$
(12)

where ρ_c is the hidden parameter that specifies instantaneous size of the yield surface and translates instantaneous combined loads into the norm of an equivalent vertical force. In order to relate size of the yield surface and incremental displacements, the hardening rule and flow rule are required. As for the hardening rule, isotropic hardening, which defines similar bearing capacity surface and yield surface, is assumed. The hardening function is expressed by

$$\rho_c = 1 - \exp\left(- \frac{R_0 v_c}{V_m} \right)$$
(13)

where R_0 is initial gradient of the $V - v^{pl}$ curve. Here, v_c is expressed by

$$v_c = \left\{ (v^{pl})^2 + (\alpha_M u^{pl})^2 + (\gamma_M B \theta^{pl})^2 \right\}^{0.5}$$
(14)

where α_M and γ_M are non-dimensional parameters that incorporate the contribution of horizontal displacement and rotation into hardening. As for the flow rule, a non-associated flow rule is adopted. Regarding such a non-associated flow rule, a plastic potential function is defined as follows:

$$g = \lambda^2 h^2 + \chi^2 m^2 - \xi^2 (1 - \xi / \rho_g)^{2\zeta} = 0$$
(15)

where $\lambda = \mu / \mu_g$, $\chi = \phi / \phi_g$, μ_g and ϕ_g are parameters that specify the shape of the plastic potential surface.

3. STRESS REDUCTION AGAINST AN ACTUAL EARTHQUAKE

Here, stress reduction effects of a structure-foundation-soil system against real earthquakes are reviewed. The system was subjected to different types of acceleration-time histories. A foundation-soil system is modeled as four cases, and it's stress reduction of piers is discussed.

3.1 Structure-Foundation-Soil System

A schematic and parameters of the structure-foundation-soil system are shown in Fig. 3 and Table 1. A superstructure was modeled by a lumped mass and Bernoulli-Euler beam. The total degrees of freedom of the system were six; consisting of three degrees of lumped mass and three degrees of the macro-element. A foundation-soil system is modeled as four cases; (1) fixed base, (2) elastic soil, (3) elastic soil with basemat uplift and (4) elasto-plastic soil with basemat uplift. The damping coefficient of the beam element was assumed to be proportional to the element stiffness matrix and 5% of the damping coefficient was taken into account. Frequency dependence of elastic compliances of the macro-element was ignored. Damping coefficients of the macro-element corresponding to the vertical, translational, and rocking component were set based on Gazetas [7]. Parameters of yield function, plastic potential and hardening function were set based on Nova and Montrasio [8] and Nakatani *et al*. [5].

3.2 Stress Reduction against an Actual Earthquake

In this section, degree of stress reduction effects of a structure is studied. The aforementioned structure-foundation-soil system is subjected to input motions in the time domain. Two kinds of ground motions are considered as the input motions here; subduction-type earthquake (acceleration time history which was recorded at a port in Hachinohe during the 1968 Tokachi-Oki Earthquake) and inland-type earthquake (acceleration time history observed at JR Takatori station during the 1995 Hyogoken-Nanbu Earthquake). These time histories are shown in Fig. 4 and 5. For conducting nonlinear analysis with the macro-element model, time step for seismic response analysis was set at 0.0001 seconds by interpolating the input time histories which were originally recorded at 0.02 second intervals. Linear

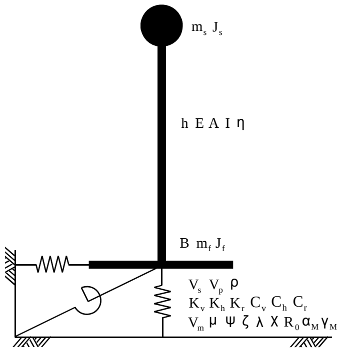

Fig. 3 Schematic diagram of structure-foundation-soil system

Table 1 Parameters of structure-foundation-soil system

Parameter	Value
Lumped mass m_s (t)	500
Moment of inertia of the structure J_s (t・m^2)	4167
Height h (m)	10
Young modulus E (kN/m^2)	2450000
Section area A (m^2)	4.423
Second moment of area I (m^4)	1.557
Damping coefficient of the structure η	0.05
Footing length B (m)	10
Mass of the foundation m_f (t)	100
Moment of inertia of the foundation J_f (t・m^2)	833
Shear wave velocity V_s (m/s)	230
Lysmer's analog wave velocity V_{La} (m/s)	356
Ground density ρ (t/m^3)	1.603
Vertical elastic spring coefficient K_v (kN/m)	2750000
Translational elastic spring coefficient K_h (kN/m)	2240000
Rocking elastic spring coefficient K_r (kN・m/rad)	5450000
Vertical damping coefficient C_v (kN・s/m)	52500
Translational damping coefficient C_h (kN・s/m)	36900
Rocking damping coefficient C_r (kN・s・m)	99800
Bearing capacity of centered vertical loading V_m (kN)	96100
Parameter of yield function μ	0.9
Parameter of yield function ψ	0.48
Parameter of yield function ζ	0.95
Parameter of plastic potential λ	0.45
Parameter of plastic potential χ	0.45
Parameter of hardening function R_0	48946
Parameter of hardening function α_M	2.8
Parameter of hardening function γ_M	1.7

acceleration method was used for the numerical integration. The time history of base shear that

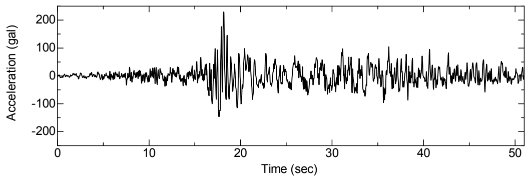

Fig. 4 Acceleration time history

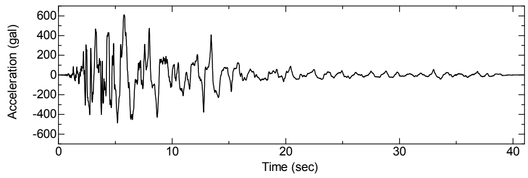

Fig. 5 Acceleration time history

occurred in the structure for subduction zone type earthquake is shown in Fig. 6. The thin black dotted-line, the thin gray line, the thick black dot-line and the thick gray line correspond to responses for fixed base case, elastic soil case, elastic soil with basemat uplift case and elasto-plastic soil with basemat uplift case, respectively. Case (1) shows time response different from other cases; and this difference implies the wave radiation effect. However, linear cases and nonlinear cases show similar time responses. This means that stress reduction effect due to basemat uplift is significant, and soil yielding are not apparent in these cases.

Secondly, an inland-type earthquake is considered as input motion into the system. Calculated responses are shown in Fig. 7. Meanings of curves are the same as in Fig. 6. Responses show significantly different waveforms. The fixed base case and elastic soil case show similar time responses (this difference implies the wave radiation effect). However, when basemat uplift is considered, base shear becomes significantly different from linear cases. Nonlinear cases show drastic reduction of base shear, thus longer period motions are implied. When soil yielding is considered, the period of the motion becomes even longer.

We can recognize from these results that stress reduction of structures due to basemat uplift and soil yielding can occur in some cases depending on input ground motions. In order to examine factors that might bring about differences in the level of stress reduction, some artificial input motions that have different frequency characteristics are considered in the next section.

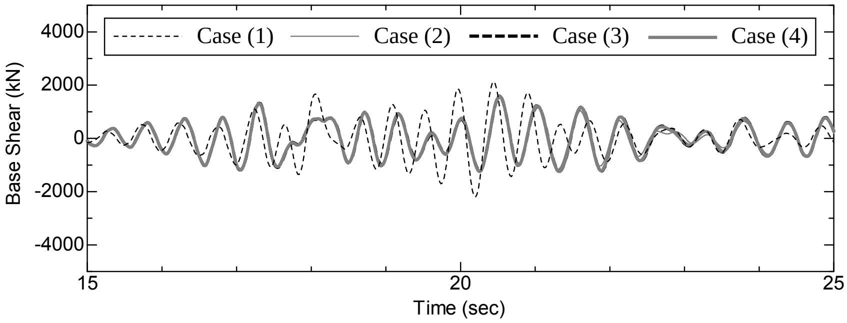

Fig. 6 Base shear time history

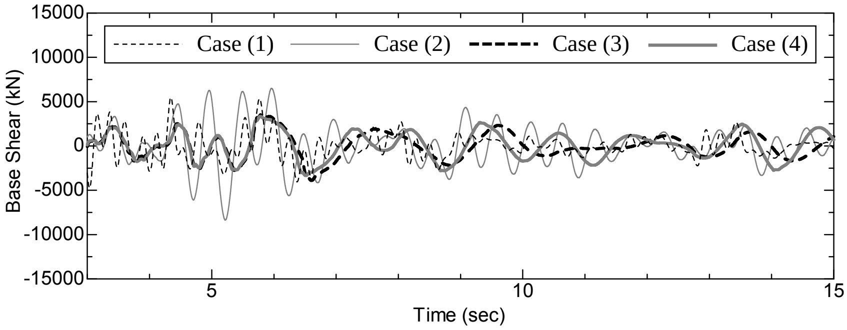

Fig. 7 Base shear time history

4. STRESS REDUCTION OF STRUCTURE FOR INPUT MOTIONS OF DIFFERENT FREQUENCY CHARACTERISTICS

The same structure-foundation-soil system is considered. As the input motion, harmonic waves that have different frequency characteristics are given. An example of the harmonic seismic wave which has a natural frequency of 1.989Hz is shown in Fig. 8. The amplitude gradually increases until it reaches an amplitude of 500gal. As the former section, foundation-soil system is modeled as four cases; (1) fixed base, (2) elastic soil, (3) elastic soil with basemat uplift and (4) elasto-plastic soil with basemat uplift. Three cases with different excitation frequencies are considered: (a) excitation frequency fe is lower than the natural frequency of the elastic soil system fn (fe/fn=0.9) (b) excitation frequency is the same as the natural frequency of the elastic soil system (fe/fn=1.0) (c) excitation frequency is higher than the natural frequency of the elastic soil system (fe/fn=1.1). The natural frequency of the elastic soil system is 1.989(Hz).

4.1 Stress Reduction for Case (a)

The time history of base shear induced in the structure is shown in Fig. 9. The meanings of the curves are the same as before. Base shear responses of fixed base and elastic soil model are larger than nonlinear cases. When basemat uplift effect is incorporated in the model, base shear reduced significantly. No clear difference can be seen by the soil yielding effect.

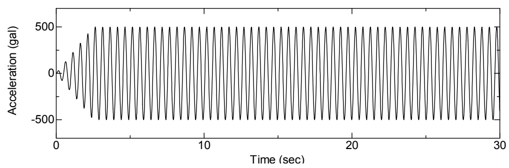

Fig. 8 Acceleration time history

4.2 Stress Reduction for Case (b)

Calculated responses are shown in Fig. 10. In this case, base shear of the elastic soil model becomes much larger than others. This is because the elastic soil system reached resonance with excitation frequency becoming system frequency. Compared to the elastic soil case, base shear of the models that incorporated basemat uplift effect showed significant reduction.

4.3 Stress Reduction for Case (c)

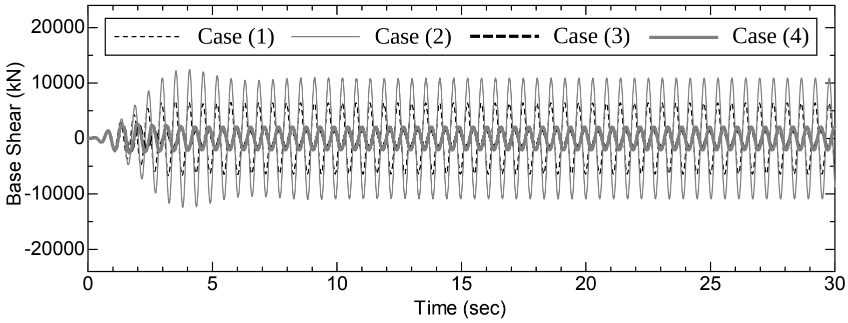

Fig. 9 Base shear time history

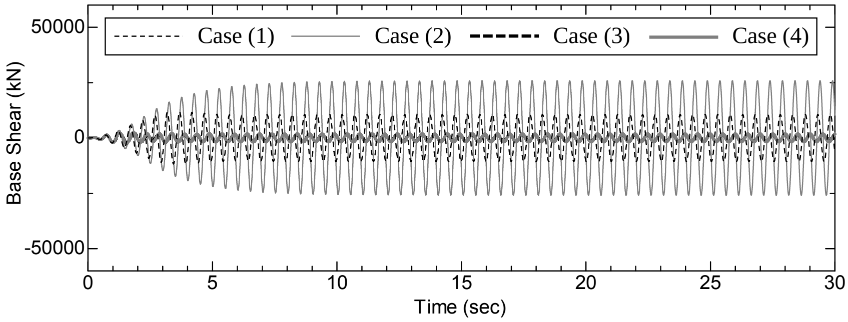

Fig. 10 Base shear time history

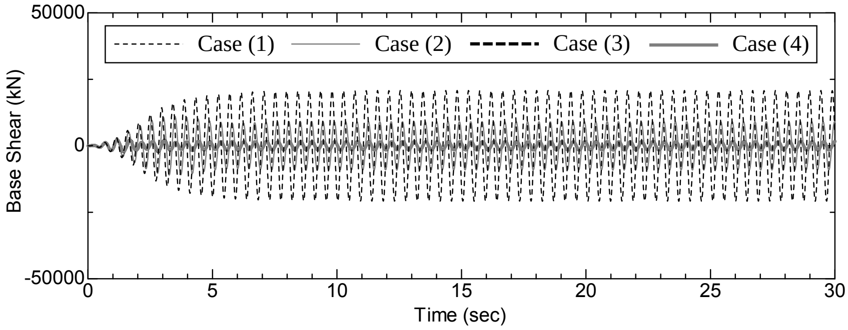

Fig. 11 Base shear time history

The results are shown in Fig. 11. In this case, excitation frequency is higher than the elastic soil system and closer to the fixed base model. For this reason, base shear of the fixed base model is largest. Owing to radiation damping effect, base shear of the elastic soil model was significantly reduced. Furthermore, basemat uplift effect works to drastically reduce the base shear of the structure in this case.

5. INVESTIGATION OF STRESS REDUCTION EFFECT USING ENERGY CONCEPT

Regarding case (c) where degree of stress reduction effect was the largest in the preceding chapter, energy balance for the system is estimated. Various energy terms can be defined by integrating the equation of motion into the system. If the macro-element model developed by Nakatani *et al.* [5] is employed, the equation of motion of the system is expressed by

$$[M]\{\ddot{u}\}+[C]\{\dot{u}\}+[K]\{u\}+\{F\}=\{P\} \quad (16)$$

where $[M]$ is the mass matrix, $[C]$ is the damping matrix, $[K]$ is the stiffness matrix for a pier, $\{F\}$ is the soil reaction force matrix from macro-element, and $\{P\}$ is the external force matrix.

Hence, the various energy terms can be expressed by

$$\int_0^t \{\dot{u}\}^T [M]\{\ddot{u}\}dt + \int_0^t \{\dot{u}\}^T [C]\{\dot{u}\}dt + \int_0^t \{\dot{u}\}^T [K]\{u\}dt + \int_0^t \{\dot{u}\}^T \{F\}dt = \int_0^t \{\dot{u}\}^T \{P\}dt \quad (17)$$

The right side of this equation is energy input to the system. The first term on the left side is kinetic energy of the system associated with its motion relative to the ground. The second term on the left side is energy dissipated by viscous damping. The third term on the left side is the potential energy of the structure. The fourth term on the left side of this equation is the potential energy of the soil. The time histories of energy for the systems are shown in Fig. 12. In this case, the input energy imparted to the structure by an earthquake tends to be smaller due to the effect of basemat uplift.

6. CONCLUSIONS

This study examined the reduction effect of a section force induced in structures due to basemat uplift and soil yielding from a viewpoint of energy concept. A macro-element model developed by PWRI which can deal with basemat uplift is used. The foundation-soil system was modeled as four cases; (1) fixed base, (2) elastic soil, (3) elastic soil with basemat uplift and (4) elasto-plastic soil with basemat uplift. Time histories with different frequency characteristics were considered as input motions in the models. Comparisons of responses

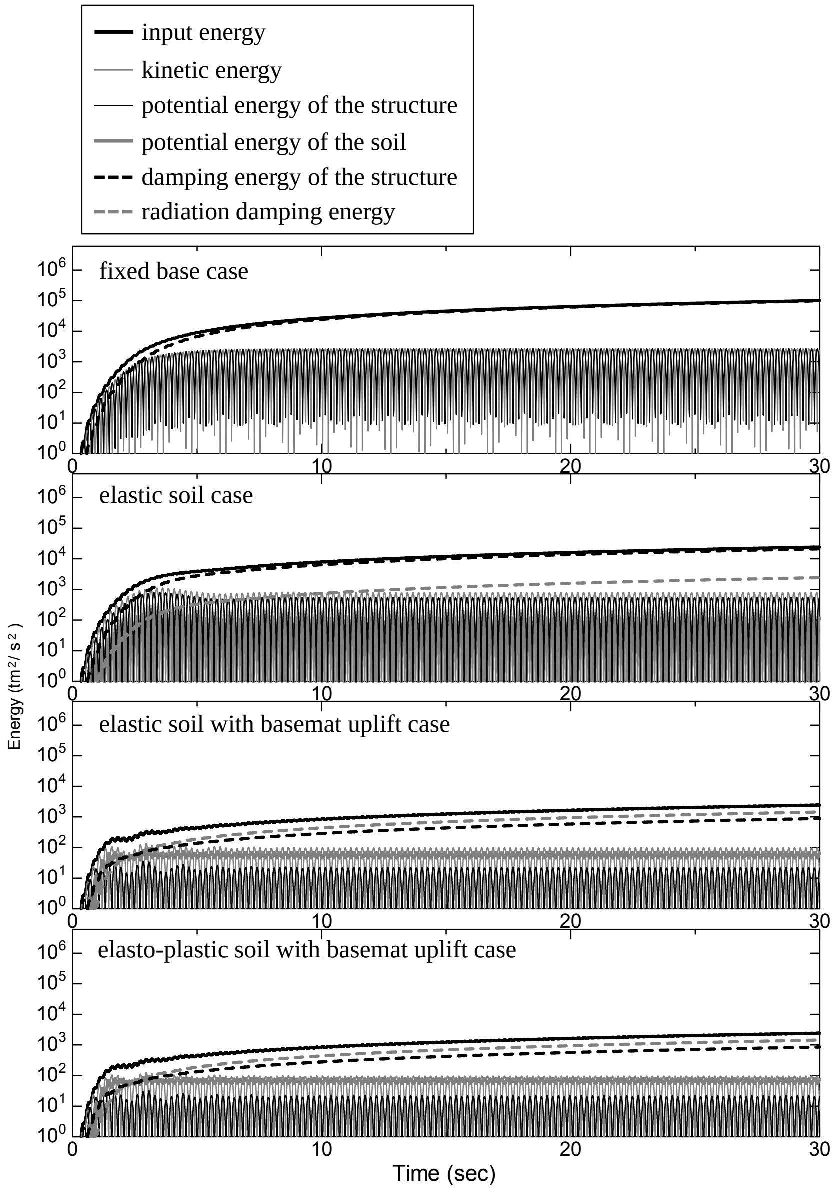

Fig. 12 Energy time history (Case (c))

for the models showed remarkable reduction of section force due to basemat uplift and soil yielding. Therefore, it may be concluded that the degree of base shear reduction depends on frequency characteristics of input motions relative to the system. Regarding the case where degree of stress reduction effect was the largest, energy flow for the system was estimated. In this case, the input energy imparted to the structure by an earthquake tended to be reduced due to the effect of basemat uplift.

7. ACKNOWLEDGEMENTS

The authors express their gratitude to the Public Works Research Institute, Tsukuba, Japan, for providing the analysis program.

8. REFERENCES

[1] Fukui J, Kimura Y, Ishida M and Kishi Y, "An investigation on the response of shallow foundations to large earthquakes", Technical Memorandum of PWRI, Public Works Research Institute, (3627), 1999, (in Japanese).

[2] Hayashi Y, "Damage reduction effect due to basemat uplift of buildings", Journal of Structural and Construction Engineering (Transactions of AIJ), 485, 1996, pp. 53-62, (in Japanese).

[3] Iwashita K, Taniguchi H, Ishihara T, "Energy Approach to the Earthquake Response of Building Allowing Uplift at Pile Head" Journal of Structural and Construction Engineering (Transactions of AIJ), 564, 2003, pp. 23-30, (in Japanese).

[4] Inoue T, and Mikami A, "Stress Reduction Effect of Structure due to Basemat Uplift and Soil Yielding," In: Proceedings of the 10th International Conference on Urban Earthquake Engineering, Tokyo, JAPAN, 2013.

[5] Nakatani S, Shirato M, and Kouno T, "Development of a numerical model for the seismic nonlinear behavior and irreversible displacement of a shallow foundations" PWRI Report, Public Works Research Institute, (4101), 2008, (in Japanese).

[6] Shirato M, Paolucci R, Kouno R, Nakatani S, Fukui J, Nova R, di Prisco C, "Numerical simulation of model tests of pier-shallow foundation systems subjected to earthquake loads using an elasto-uplift-plastic macro element" Soils and Foundations, 48(5), 2008, pp. 693-71.

[7] Gazetas G, "Foundation vibrations" Foundation Engineering Handbook, Fang HY (ed.), van Nostrand Reinhold: NY, 1991.

[8] Nova R, and Montrasio L, "Settlement of shallow foundations on sand," Géotechnique, 41(2), 1991, pp. 243-256.

Int. J. of GEOMATE, March, 2014, Vol. 6, No. 1 (Sl. No. 11), pp. 749-756.

MS No. 3267 received on June 16, 2013 and reviewed under GEOMATE publication policies.
Copyright © 2014, International Journal of GEOMATE. All rights reserved, including the making of copies unless permission is obtained from the copyright proprietors.
Pertinent discussion including authors' closure, if any, will be published in the March. 2015 if the discussion is received by Sept, 2014.
Corresponding Author: Takafumi Inoue